Steel and Composite Structures, *Vol. 27, No. 1 (2018) 13-25*
DOI: https://doi.org/10.12989/scs.2018.27.1.013

A dual approach to perform geometrically nonlinear analysis of plane truss structures

AliReza Habibi [*1] and Shaahin Bidmeshki [2a]

[1] *Department of Civil Engineering, Shahed University, Tehran, Iran*
[2] *Department of Civil Engineering, University of Kurdistan, Sanandaj, Iran*

(*Received July 13, 2017, Revised November 20, 2017, Accepted January 21, 2018*)

Abstract. The main objective of this study is to develop a dual approach for geometrically nonlinear finite element analysis of plane truss structures. The geometric nonlinearity is considered using the Total Lagrangian formulation. The nonlinear solution is obtained by introducing and minimizing an objective function subjected to displacement-type constraints. The proposed method can fully trace the whole equilibrium path of geometrically nonlinear plane truss structures not only before the limit point but also after it. No stiffness matrix is used in the main approach and the solution is acquired only based on the direct classical stress-strain formulations. As a result, produced errors caused by linearization and approximation of the main equilibrium equation will be eliminated. The suggested algorithm can predict both pre- and post-buckling behavior of the steel plane truss structures as well as any arbitrary point of equilibrium path. In addition, an equilibrium path with multiple limit points and snap-back phenomenon can be followed in this approach. To demonstrate the accuracy, efficiency and robustness of the proposed procedure, numerical results of the suggested approach are compared with theoretical solution, modified arc-length method, and those of reported in the literature.

Keywords: plane truss; geometric; nonlinear finite element; total Lagrangian; dual approach; snap-through

1. Introduction

Normally, steel structures are very practical in the construction industry. Although the fundamental theory of structural analysis and linear elastic formulations are typically used for analysis and design of these structures, they may undergo large deformations under abnormal situations before reaching their limit of resistance. Therefore, nonlinear analysis must be done to predict the real behavior of steel structures. There are two types of nonlinearities in structural analysis, namely; material nonlinearity and geometric nonlinearity. In this study, geometric nonlinear analysis and entire aspects of the nonlinear equilibrium path of the plane truss structures are considered. To study the real behavior of the truss structures, the both pre- and post-buckling regions of equilibrium path must be traced including limit points, snap-through and snap-back phenomena. Crisfield (1991) described important reasons why tracing of the whole equilibrium path and its features are essential. Due to the importance of this subject, it has been extensively studied by many researchers. The interested reader may find more information about different kinds of nonlinear finite element analysis in Garcea *et al*. (2009), Pastor *et al*. (2013), Liang *et al*. (2014), Rezaiee-Pajand *et al*. (2014), Izadpanah and Habibi (2015), Alnaas and Jefferson (2016), Jiang *et al*. (2016), Wan and Zha (2016), and Rezaiee-Pajand and Naserian (2017).

There are several numerical methods to solve nonlinear equilibrium equations. Among them incremental-iterative solution methods are very popular and widely used to follow the equilibrium path. They can be classified as: the load-controlled methods (Newton-Raphson methods), displacement-controlled methods, generalized displacement-controlled method, arch-length method, and work-controlled methods (Torkamani and Sonmez 2008). The load-controlled and displacement-controlled methods are the fundamental and earliest methods. Many procedures and different algorithms have been offered to develop these two initial methods. The other incremental-iterative methods are considered as advanced methods and have been developed based on the two mentioned fundamental methods. Each of the iterative-incremental methods has its own benefits and limitations (Thai and Kim 2009).

The load-controlled methods are used to trace load-deflection curve of engineering structures only prior to the critical load. If the applied external load exceeds the load-carrying capacity of structure, the convergence fails (Torkamani and Sonmez 2008). As a result, load-controlled methods cannot be used for following the equilibrium path of the structures beyond the critical load point (Chen and Lui 1991 and Yang and Kuo 1994), however, they are still widely used in nonlinear analysis of structures (Saffari and Mansouri 2011, Saffari *et al*. 2012, Mansouri and Saffari 2012, Mahdavi *et al*. 2015 and Hamdaoui *et al*. 2016).

One of the most popular incremental-iterative solution methods to perform nonlinear analysis of structures is the

*Corresponding author, Ph.D., Associate Professor,
E-mail: ar.habibi@shahed.ac.ir
[a] Ph.D. Student, E-mail: sh.bidmeshki@gmail.com

ISSN: 1229-9367 (Print), 1598-6233 (Online)

arc-length method which is extensively used since it was first introduced by Wempner (1971), Riks (1972) and Riks (1979). Ramm (1981), Crisfield (1981), Bathe and Dvorkin (1983), Crisfield (1983), Schweizerhof and Wriggers (1986), Bellini and Chulya (1987), Forde and Stiemer (1987) and others have developed and improved the original method in various ways. It is possible to follow the whole equilibrium path of structures using the arc - length methods. They are categorized as the cylindrical and the spherical arc-length methods. Numerical obstacles can be observed in both types of these methods in the vicinity of limit points with severe snap-back phenomenon (Geers 1999). Hellweg and Crisfield (1998) proposed an improved and modified arc-length method to pass the limit points associated with severe snap-back phenomenon. According to Geers (1999), the modified arc-length method, proposed by Hellweg and Crisfield (1998), has not been successful to solve these numerical difficulties, yet.

In this paper, a dual approach is suggested to solve geometrically nonlinear finite element equations of plane truss structures. This approach uses classical nonlinear finite element formulation to establish an objective function and nonlinear programming techniques as a search method. Our approach does not establish any stiffness matrix derived by linearization and is formed only by using classical stress-strain formulation. As a result, errors due to the linearization and neglecting some of the nonlinear incremental strain components, and higher-order terms will be excluded. The proposed algorithm can also trace nonlinear region of a load-displacement curve beyond the limit point accompanied by exhibiting snap-through and snap-back phenomena. Furthermore, utilizing optimization techniques, the convergence of the analysis and reducing the number of required repeated analyses are guaranteed. To demonstrate the capability of the proposed approach, five numerical examples are investigated, and the acquired results are compared to modified arc-length method, and the outcomes of benchmark problems.

2. The incremental-iterative method

There are several methods to trace equilibrium path, including load-controlled, displacement-controlled and ANM (Asymptotic Numerical Method) techniques (Damil and Potier-Ferry 1990, Elhage-Hussein *et al*. 2000, Baguet and Cochelin 2003 and Hamdaoui *et al*. 2016). Both load-controlled and displacement-controlled methods will fail in the vicinity of turning points that are known as “snap-through” for load-controlled method and “snap-back” for displacement-controlled method (see Figs. 1(a) and (b)). These difficulties usually occur in buckling analysis of steel structures. An ideal solution method must be able to successfully overcome these difficulties and also be stable for all possible nonlinear behaviors, including softening, hardening as well as having numerical stability at the limit points (see Fig. 1(c)).

In order to follow the whole equilibrium path, all particles of the body should be traced in their motion, from the original to the final configuration of the body, which is named Lagrangian formulation. In practice, three types of Lagrangian kinematic formulation are employed for finite

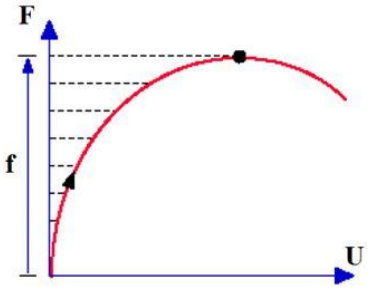

(a) Failure of load control

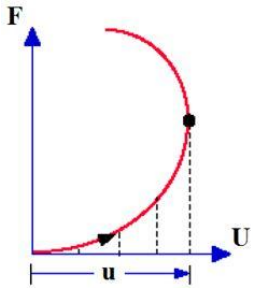

(b) Failure of displacement control

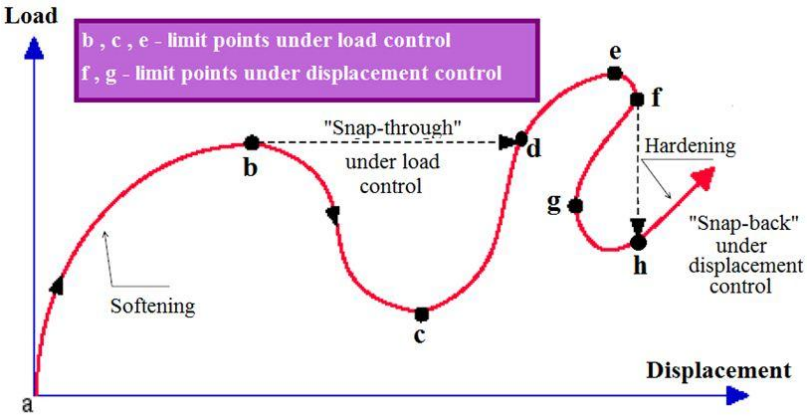

(c) Characteristics of nonlinear equilibrium path

Fig. 1 General characteristics of nonlinear systems

element analysis of geometrically nonlinear structures namely: (1) Total Lagrangian (TL) formulation; (2) Updated Lagrangian (UL) formulation; and (3) co-rotational formulation (Crisfield 1991, Felippa 2001, Saada 2013 and Liang *et al*. 2016). The TL formulation is selected in this study. In the TL description, the initial configuration of the element at time 0 is considered as a reference configuration and all static and kinematic quantities are referred to this configuration. The TL formulation can reflect all kinematic nonlinear effects due to large deformations, and large strains, but large strain behavior is modeled correctly if appropriate constitutive relations are specified.

In Total Lagrangian incremental analysis approach, the equilibrium equation at time $t+\Delta t$ is introduced using the principle of virtual displacements as follows (Bathe 2006)

$$\int_{{}^0V} {}^{t+\Delta t}S_{ij}\ \delta\,{}^{t+\Delta t}_{0}\varepsilon_{ij_g}\ d\,{}^0V = {}^{t+\Delta t}R \tag{1}$$

Where ${}^{t+\Delta t}_{0}S_{ij}$, $\delta\,{}^{t+\Delta t}_{0}\varepsilon_{ij_g}$, ${}^{t+\Delta t}R$, and ${}^0V$ are the second Piola-Kirchhoff stress components, the Green-Lagrange strain components corresponding to virtual displacements, the external virtual work at time t, and the volume at time 0, respectively. Generally, ${}^{t+\Delta t}R$ is dependent on the volume of the body and the surface area. In this study, however, the external virtual work generated by concentrated forces whose intensities and directions are irrelevant to the deformations (Bathe 2006). ${}^{t+\Delta t}_{0}S_{ij}$, ${}^{t+\Delta t}_{0}\varepsilon_{ij_g}$, and $\delta\,{}^{t+\Delta t}_{0}\varepsilon_{ij_g}$ are decomposed as

$${}^{t+\Delta t}_{0}S_{ij} = {}^{t}_{0}S_{ij} + {}_0S_{ij} \tag{2}$$

$${}^{t+\Delta t}_{0}\varepsilon_{ij_g} = {}^{t}_{0}\varepsilon_{ij_g} + {}_0\varepsilon_{ij_g} \tag{3}$$

$$\begin{aligned}\delta\,{}^{t+\Delta t}_{0}\varepsilon_{ij_g} &= \delta\left({}^{t}_{0}\varepsilon_{ij_g} + {}_0\varepsilon_{ij_g}\right)\\ &= \underbrace{\delta\,{}^{t}_{0}\varepsilon_{ij_g}}_{0} + \delta\ {}_0\varepsilon_{ij_g} = \delta\ {}_0\varepsilon_{ij_g}\end{aligned} \tag{4}$$

Where ${}^{t}_{0}S_{ij}$ denote the second Piola-Kirchhoff stress components at time *t*, ${}_0S_{ij}$ the increment of second Piola-Kirchhoff stress components, ${}^{t}_{0}\varepsilon_{ij_g}$ the second Piola-Kirchhoff stress components at time t, and ${}_0\varepsilon_{ij_g}$ the increment of Green-Lagrange strain components. Additionally, ${}_0\varepsilon_{ij_g}$ is decomposed as

$${}_0\varepsilon_{ij_g} = {}_0e_{ij} + {}_0\eta_{ij} \tag{5}$$

Where ${}_0e_{ij}$ and ${}_0\eta_{ij}$ are the linear and nonlinear incremental strains referred to the initial configuration. They are written as

$${}_0e_{ij} = \frac{1}{2}({}_0u_{i,j} + {}_0u_{j,i} + {}^{t}_{0}u_{k,i}\,{}_0u_{k,j} + {}_0u_{k,i}\,{}^{t}_{0}u_{k,j}) \tag{6}$$

$${}_0\eta_{ij} = \frac{1}{2}\,{}_0u_{k,j}\,{}_0u_{k,i} \tag{7}$$

Where

$$\begin{aligned}{}_0u_{i,j} &= \frac{\partial u_i}{\partial\,{}^0x_j}\\ {}^{t}_{0}u_{k,i} &= \frac{\partial\,{}^{t}u_k}{\partial\,{}^0x_i}\end{aligned} \tag{8}$$

Hence, we have

$$\begin{aligned}&\int_{{}^0V}\left({}^{t}_{0}S_{ij} + {}_0S_{ij}\right)\delta\ {}_0\varepsilon_{ij_g}\,d\,{}^0V = {}^{t+\Delta t}R\\ &\rightarrow \int_{{}^0V}{}^{t}_{0}S_{ij}\,\delta\ {}_0\varepsilon_{ij_g}\,d\,{}^0V + \int_{{}^0V}{}_0S_{ij}\,\delta\ {}_0\varepsilon_{ij_g}\,d\,{}^0V = {}^{t+\Delta t}R\\ &\rightarrow \int_{{}^0V}{}^{t}_{0}S_{ij}\,\delta\ {}_0e_{ij}\,d\,{}^0V + \int_{{}^0V}{}^{t}_{0}S_{ij}\,\delta\ {}_0\eta_{ij}\,d\,{}^0V\\ &\quad + \int_{{}^0V}{}_0S_{ij}\,\delta\ {}_0\varepsilon_{ij_g}\,d\,{}^0V = {}^{t+\Delta t}R\\ &\rightarrow \int_{{}^0V}{}^{t}_{0}S_{ij}\,\delta\ {}_0\eta_{ij}\,d\,{}^0V + \int_{{}^0V}{}_0S_{ij}\,\delta\ {}_0\varepsilon_{ij_g}\,d\,{}^0V\\ &\quad = {}^{t+\Delta t}R - \int_{{}^0V}{}^{t}_{0}S_{ij}\,\delta\ {}_0e_{ij}\,d\,{}^0V\end{aligned} \tag{9}$$

It should be noted that the term $\int_{{}^0V}^{t} S_{ij}\,\delta_0 e_{ij}\,d^0V$ is known, and the term $\int_{{}^0V}^{t} S_{ij}\,\delta_0\eta_{ij}\,d^0V$ is linear with respect to the incremental displacements. But the term $\int_{{}^0V}^{t} S_{ij}\,\delta_0\eta_{ij}\,d^0V$ is highly nonlinear with respect to the incremental displacements u_i, therefore, this term is linearized using Taylor series expansion as follows

$$\begin{aligned}&\int_{{}^0V}{}_0S_{ij}\,\delta\ {}_0\varepsilon_{ij_g}\,d\,{}^0V\\ &= \int_{{}^0V}\left(\frac{\partial\,{}^{t}_{0}S_{ij}}{\partial\,{}^{t}_{0}\varepsilon_{rs}}\Big|_t\ {}_0\varepsilon_{rs} + higher\ order\ terms\right)\\ &\qquad \delta\left({}_0e_{ij} + {}_0\eta_{ij}\right)d\,{}^0V\\ &= \int_{{}^0V}\Big(\underbrace{\frac{\partial\,{}^{t}_{0}S_{ij}}{\partial\,{}^{t}_{0}\varepsilon_{rs}}\Big|_t}_{{}_0C_{ijrs}}\Big({}_0e_{rs} + \underbrace{{}_0\eta_{rs}}_{Neglect}\Big)\\ &\qquad + \underbrace{higher\ order\ terms}_{Neglect}\Big)\delta\Big({}_0e_{ij} + \underbrace{{}_0\eta_{ij}}_{Neglect}\Big)\,d\,{}^0V\\ &= \int_{{}^0V}{}_0C_{ijrs}\ {}_0e_{rs}\,\delta\ {}_0e_{ij}\,d\,{}^0V\end{aligned} \tag{10}$$

Where, ${}_0C_{ijrs}$ is the incremental stress-strain tensor. It

should be stated that nonlinear incremental components of strain, and higher order terms have been neglected in Eq. (10). Accordingly, the linearized equilibrium equation is written as

$$\int_{{}^0V} {}_0C_{ijrs}\ {}_0e_{rs}\ \delta\,{}_0e_{ij}\ d\,{}^0V + \int_{{}^0V} {}^t_0S_{ij}\ \delta\,{}_0\eta_{ij}\ d\,{}^0V = {}^{t+\Delta t}R - \int_{{}^0V} {}^t_0S_{ij}\ \delta\,{}_0e_{ij}\ d\,{}^0V \tag{11}$$

The term $\int_{{}^0V} {}_0C_{ijrs}\ {}_0e_{rs}\delta_0 e_{ij}\, d^0V$ is used to form linear stiffness matrix K_L, the term $\int_{{}^0V} {}^t_0S_{ij}\,\delta_0\eta_{ij}\, d^0V$ to form nonlinear stiffness matrix K_{NL}, and the term $\int_{{}^0V} {}^t_0S_{ij}\,\delta_0 e_{ij}\, d^0V$ to form the vector of internal nodal forces F. Therefore, the linearized terms are used to determine approximated stiffness matrix, internal nodal forces, and then incremental displacements, strains and stresses. Therefore, the accumulative errors may lead to an incorrect solution. Furthermore, it will be deteriorated in the case of highly nonlinear behavior. The error due to the linearization, neglecting some of the nonlinear incremental strain components, and higher-order terms of the original TL formulation can be expressed as

$$Error = {}^{t+\Delta t}R - \int_{{}^0V} {}^{t+\Delta t}_0S^{(1)}_{ij}\ \delta\,{}^{t+\Delta t}_0\varepsilon^{(1)}_{ij_g}\ d\,{}^0V \tag{12}$$

The superscript (1) indicates approximated value. Eq. (12) is considered as "unbalanced virtual work" (Bathe 2006). In order to further reducing "unbalanced virtual work" in incremental-iterative methods, an iterative process must be performed until the difference between the external virtual work and the internal virtual work satisfies a desired convergence value.

3. Proposed approach

The external virtual work is relevant to external loading and is usually constant for a virtual displacement pattern, but the internal virtual work is dependent on real displacements. Therefore, to eliminate computational errors due to linearization of the nonlinear terms of the equilibrium equation, neglecting some of the nonlinear incremental strain components and higher-order terms, and derivation of the approximated stiffness matrices, the nonlinear response at each arbitrary time is directly determined by using classical stress-strain formulation, and constrained optimization techniques simultaneously.

3.1 Main objective function

In this study, to solve nonlinear equilibrium equation of the structures, the following optimization problem is defined as an error formula

$$\begin{aligned} &\textit{Minimize}\ \ \mathrm{W}_1 = \frac{\|R_e - F\|_2}{1+\|R_e\|_2} \\ &\textit{subjected}\ \ \text{to}\ \ \mathrm{u}_{iL} \le u_i \le u_{iU} \end{aligned} \tag{13}$$

Where R_e is the vector of concentrated loads (irrelevant to the direction and intensity of the nodal displacement vector), F is the function of internal nodal forces (dependent on the nodal displacements), u_i is the global nodal displacement, u_{iL} and u_{iU} are the lower and upper bounds of displacements, respectively. The lower and upper displacements bounds are considered as constraints to overcome the common failure of load-controlled and displacement-controlled methods at the turning points (snap-through and snap-back phenomena, depicted in Fig. 1). Additionally, since the proposed optimization algorithm finds the local minimum solution, defining displacement-type constraints is necessary to distinguish the pre- and post-turning point regions. Otherwise, it may lead to jump from the pre- to the post-turning regions in the vicinity of limit points.

To formulate the objective function given in Eq. (13) with respect to the global nodal displacements, classical stress-strain formulations of nonlinear equilibrium equation based on a known displacement field are presented. The vector of updated global nodal coordinates D_{new} is stated as

$$D_{new} = D + U \tag{14}$$

Where D lists the initial global nodal coordinates, and U the vector of global nodal displacements.

The deformation of the body can be measured by the deformation gradient. The deformation gradient describes the stretches and rotations that the material fibers have undergone from time 0 to t. Generally, the deformation gradient X is presented using initial and new geometries as written in Eq. (15)

$$X = \begin{bmatrix} 1+\dfrac{\partial u}{\partial x} & \dfrac{\partial u}{\partial y} \\ \dfrac{\partial v}{\partial x} & 1+\dfrac{\partial v}{\partial y} \end{bmatrix} \tag{15}$$

Where u and v are displacement functions based on the element's shape functions and global nodal displacements in x- and y-directions, respectively.

For large deformations, different kinds of strain measures such as Green-Lagrange, Hencky, and Almansi may be employed. All mentioned strains are obtained using deformation gradient (Crisfield 1991 and Bathe 2006). However, in this research, Green-Lagrange strain measure is employed and presented in tensor form as

$$\varepsilon_g = \frac{1}{2}\left(X^T X - I\right) \tag{16}$$

Where I denotes a second order identity tensor. It should be stated that the Green - Lagrange strain is the complete strain tensor from which no higher-order terms and no nonlinear incremental strain components have been neglected. The Green-Lagrange strain is measured with respect to the initial coordinates of the body (Indeed, with respect to the undeformed configuration of the body). For each truss element, it can be defined as

$$\varepsilon_g^{(i)} = \left(\frac{L^{(i)}_{new} - L^{(i)}}{L^{(i)}}\right) + \frac{1}{2}\left(\frac{L^{(i)}_{new} - L^{(i)}}{L^{(i)}}\right)^2 \tag{17}$$

Where $\varepsilon_g^{(i)}$, $L_{new}^{(i)}$, and $L^{(i)}$ denote the Green-Lagrange strain, the new length, and the initial length of the i*th* element, respectively. Now, by using second Piola-Kirchhoff stress of the i*th* element ($S^{(i)}$) as a work-conjugate with the Green-Lagrange strain of the i*th* element, and employing an appropriate constitutive law, we have

$$S^{(i)} = C^{(i)}\ \varepsilon_g^{(i)} \tag{18}$$

Where $C^{(i)}$ is the constant elasticity modulus of the i*th* element. The internal force of each element can be specified as the following equation

$$P^{(i)} = S^{(i)}.A^{(i)}.(\frac{L_{new}^{(i)}}{L^{(i)}}) \tag{19}$$

In Eq. (19), $A^{(i)}$ is the cross-section area of each the i*th* element. Then, the vector of global internal nodal forces of the i*th* element can be described as

$$F^{(i)} = \begin{bmatrix} -C_x^{(i)} \\ -C_y^{(i)} \\ C_x^{(i)} \\ C_y^{(i)} \end{bmatrix} . P^{(i)} \tag{20}$$

Where

$$\begin{aligned} C_x^{(i)} &= \mathrm{Cos}\ \theta_x^{(i)} \\ C_y^{(i)} &= \mathrm{Cos}\ \theta_y^{(i)} \end{aligned} \tag{21}$$

In Eq. (21), $\theta_x^{(i)}$ and $\theta_y^{(i)}$ are the smallest angles between the i*th* element, and the positive *x* and *y* global axes. Finally, the vector of internal nodal forces of the elements should be assembled to obtain the global vector of internal nodal forces of the entire structure.

3.2 Direct estimation of limit points

For structures exhibiting softening behavior, the load-deflection curve becomes flatter when the load magnitude is increased. For these structures a critical load value is a load at which the structures become unstable and is said to have buckled (Bhatti 2006). The load at which this happens is called the buckling (limit) load. Common nonlinear analysis methods encounter difficulties in the vicinity of the limit points because even a small variation in the applied load may produce huge amount of displacement increments. Therefore, a prior estimation of the limit load may circumvent of these difficulties. In addition, the computed limit displacements can be used as appropriate lower and upper bound displacement constraints. At limit points, the global tangential stiffness matrix K_T is singular (Planinc and Saje 1999). It means that in this state, one of the eigenvalues of the tangent stiffness matrix K_T will be zero or a very small value. As a result, a new objective function is defined to directly estimate the buckling load and its corresponding limit points as

$$\begin{aligned} &\textit{Minimize} \quad W_1 + W_2 \\ &\textit{Subjected to}\ \ \mathrm{u}_{iL} \le u_i \le u_{iU} \\ &\qquad\qquad \mathrm{R}_{iL} \le R_i \le R_{iU} \end{aligned} \tag{22}$$

Where

$$\begin{aligned} W_1 &= \frac{\left\| R_e - F \right\|_2}{1 + \left\| R_e \right\|_2} \\ W_2 &= \min \left| eignvalues\left(K_T \right) \right| \end{aligned} \tag{23}$$

Where u_i is the limit displacement points, u_{iL} and u_{iU} are the lower and upper bounds of the displacements, R_i is the global nodal buckling load, R_{iL} and R_{iU} are the lower and upper bounds of buckling loads, respectively. W_2 is specified as the smallest absolute eigenvalue of the global tangent stiffness matrix. The tangent stiffness matrix of the i*th* element is defined as (Bathe 2006)

$$K_T^{(i)} = K_L^{(i)} + K_{NL}^{(i)} \tag{24}$$

Where $K_L^{(i)}$ and $K_{NL}^{(i)}$ denote the linear and nonlinear tangent stiffness matrix of the i*th* element, respectively. They are written as

$$K_L^{(i)} = \frac{C^{(i)}A^{(i)}\left(L_{new}^{(i)}\right)^2}{\left(L^{(i)}\right)^3} \begin{bmatrix} \left(C_x^{(i)}\right)^2 & C_x^{(i)}.C_y^{(i)} & -\left(C_x^{(i)}\right)^2 & -C_x^{(i)}.C_y^{(i)} \\ C_x^{(i)}.C_y^{(i)} & \left(C_y^{(i)}\right)^2 & -C_x^{(i)}.C_y^{(i)} & -\left(C_y^{(i)}\right)^2 \\ -\left(C_x^{(i)}\right)^2 & -C_x^{(i)}.C_y^{(i)} & \left(C_x^{(i)}\right)^2 & C_x^{(i)}.C_y^{(i)} \\ -C_x^{(i)}.C_y^{(i)} & -\left(C_y^{(i)}\right)^2 & C_x^{(i)}.C_y^{(i)} & \left(C_y^{(i)}\right)^2 \end{bmatrix} \tag{25}$$

$$K_{NL}^{(i)} = \frac{P^{(i)}}{L_{new}^{(i)}} \begin{bmatrix} 1 & 0 & -1 & 0 \\ 0 & 1 & 0 & -1 \\ -1 & 0 & 1 & 0 \\ 0 & -1 & 0 & 1 \end{bmatrix} \tag{26}$$

Finally, the global tangent stiffness of the elements should be assembled to form the global stiffness matrix of the entire structure (K_T). It should be noted that the tangent stiffness matrix (K_T) is obtained by linearization and neglecting of some nonlinear components of the strain, and higher-order terms. Nevertheless, it is used only in the estimation of the limit points to be introduced as displacement-type constraints as well as to have a deep insight of buckling load levels, and it is not employed in the main proposed objective function.

Indeed, in this objective function, two sets of variables are determined simultaneously. They are specified as nodal buckling load and its corresponding limit points (nodal displacements).

3.3 Optimization method

The task of optimization is the process in which the best result under given conditions is acquired. The major aim of the optimization process is minimizing the effort required. Since the required effort in any practical problem may be described as a function of certain decision variables,

optimization may be represented as the procedure of finding the states that produce the minimum amount of a function (Rao 2009). A nonlinear optimization problem subjected to inequality constraints is defined as

$$\begin{aligned} &\text{minimize} \quad \mathrm{W}(\mathrm{u}_i)\ ;\ \mathrm{i}=1 \text{ to } \mathrm{n} \\ &\text{subjected to;}\ g_j(u_i) \le 0\ ;\ \mathrm{j}=1 \text{ to } \mathrm{m} \end{aligned} \tag{27}$$

Where $W(u_i)$ denotes the objective function (w_1 and/or ($w_1 + w_2$) in this study), u_i the design variables (global nodal displacements), $g_j(u)$ the inequality constraints in terms of the global nodal displacements, n the number of nodal displacements, and m the number of inequality constraints. It should be noted that in this research, $W(u_i)$ and $g_j(u)$ are nonlinear and linear functions in terms of the global nodal displacements, respectively.

According to the nature of the problem, a number of procedures have been developed to solve different types of optimization problems. In this study, Sequential Quadratic Programming (SQP) method is used to solve constrained optimization problem. This method is efficient, reliable, and generally applicable (Rao 2009). Generally, the SQP method can be specified by the following steps (Arora 2012);

Step 1. Introducing initial vector of global nodal displacements U^0, and set the number of current iteration $k = 0$. Choosing an initial value for penalty parameter R_0 (i.e., $R_0 = 1$), and two small values of $\epsilon_1 > 0$ and $\epsilon_2 > 0$ that describe the allowable convergence parameter and constraint violation values, respectively.

Step 2. Determination of the both objective and inequality constraint functions, and their gradient values at U^k (where U^k is the vector of global nodal displacements at the k*th* iteration).

Step 3. Computation of the maximum constraint violation V_k at the vector of global nodal displacements $U^{(k)}$ as;

$$V_k = \max\{0\ ;\ \mathrm{g}_1, g_2, \ldots, g_m\} \tag{28}$$

Where g_m is the m*th* inequality constraint violation.

Step 4. The objective function $W(u_i)$ is approximated with a new Quadratic Programming (QP) subproblem subjected to the linearized inequality constraints as Eq. (29). It should be stated that the linearized inequality constraints employed in the QP problem agree well with the linearized displacement-type constraints defined in Eq. (27). Hence, the linear approximation of the inequality constraints is not required. As a result, the rate of convergence is increased. Now, the QP subproblem is minimized to find the search direction vector d, and the vector of Lagrange multipliers $\lambda^{(k)}$

$$\begin{aligned} &\text{minimize} \quad \overline{f} = c^T d + \frac{1}{2} d^T H\ d \\ &\textit{subjected}\ \text{ to} \quad A^T d \le b \end{aligned} \tag{29}$$

Where $\bar{f}$ is the quadratic approximation of the error formula defined in Eq. (13), and also we have

$$c^T d = \sum_{i=1}^{n} c_i d_i \tag{30}$$

$$c_i = \frac{\partial W(u^k)}{\partial u_i} \quad ;\ \mathrm{i}=1 \text{ to } \mathrm{n} \tag{31}$$

(n=the number of variables)

$$d_i = \Delta u_i^{(k)}\ ;\ d = \Delta U^k \tag{32}$$

$$\sum_{i=1}^{n} a_{i,j} d_i \le b_j\ ;\ j = 1\ to\ m\ \ (A^T d \le b) \tag{33}$$

$$a_{i,j} = \frac{\partial g_j(u^{(k)})}{\partial u_i} \tag{34}$$

$$b_j = -g_j(u^{(k)}) \tag{35}$$

$$L = \overline{f} + \sum_{j=1}^{m} \lambda_j g_j \tag{36}$$

$$H = \begin{bmatrix} \frac{\partial^2 L}{\partial u_1^2} & \frac{\partial^2 L}{\partial u_1 \partial u_2} & \cdots & \frac{\partial^2 L}{\partial u_1 \partial u_n} \\ \frac{\partial^2 L}{\partial u_2 \partial u_1} & \frac{\partial^2 L}{\partial u_2^2} & \cdots & \frac{\partial^2 L}{\partial u_1 \partial u_n} \\ \vdots & \vdots & \ddots & \vdots \\ \frac{\partial^2 L}{\partial u_n \partial u_1} & \cdots & \cdots & \frac{\partial^2 L}{\partial u_n \partial u_n} \end{bmatrix} \tag{37}$$

Where H is the Hessian matrix of the Lagrangian function L.

Step 5. Checking the convergence (stop) criterion $\|d\|_2 \le \epsilon_1$ ($\|d\|_2$ is norm of the search direction), and the maximum constraint violation $V_k \le \epsilon_2$. If they are satisfied, $U^{(k)}$ is the solution. Otherwise, continue.

Step 6. If $k = 0$, then $H^{(0)} = I$ (where I is the identity matrix). If $k > 0$, updating the Hessian matrix using modified Broyden-Fletcher-Goldfarb-Shanno (BFGS) formula (Powell 1978).

Step 7. Introducing a descent function by adding a penalty for constraint violations to the current value of the objective function. In this study, Pshenichny's descent function is employed due to its efficiency and robustness (Belegundu and Arora 1984b, a). The Pshenichny's descent function Φ at the point $U^{(k)}$ is computed as

$$\Phi_k = f_k + R V_k \tag{38}$$

Where f_k is the amount of objective function at the point $U^{(k)}$, R the current value of penalty parameter obtained by Eq. (39), and V_k the maximum constraint violation defined in Eq. (28).

$$R = \max(R_k, r_k) \tag{39}$$

Where

$$r_k = \sum_{i=1}^{m} \lambda_i^{(k)} \tag{40}$$

Step 8. Set $U^{(k+1)} = U^{(k)} + \alpha_k d^{(k)}$ to update the global nodal displacements, where $\alpha = \alpha_k$ is an appropriate step size along the search direction. It is acquired by minimizing the Pshenichny's descent function along the search direction $d^{(k)}$ in a way that a sufficient decrease in the descent function is obtained.

Step 9. Updating the iteration number $k = k + 1$, and go to step 2.

4. Nonlinear solution algorithm

The application of the proposed approach developed in this study is facilitated by the following algorithm:

(1) Introduce mechanical and geometrical properties of the structure
(2) Introduce the buckling (critical) loads and their corresponding nodal displacements obtained from Eq. (22) or based on the structure's inherent
(3) Introduce a desired tolerance for convergence criteria
(4) Choose an arbitrary load step λ and define computed buckling load as $R_{buckling}$. And then, $R^{(i+1)} = R^{(i)} + \lambda \leq R_{buckling}$
(5) Introduce the first lower and upper bounds of nodal displacements u_{iL} and u_{iU} as the displacement-type constraints
(6) Introduce the initial nodal displacement vector U for the optimization problem defined in Eq. (13)
(7) Update the geometry of the global nodal coordinates using Eq. (14)
(8) Calculate the new length of each element $L_{new}^{(i)}$
(9) Calculate Green-Lagrange strain of each element using Eq. (17)
(10) Calculate second Piola-Kirchhoff stress $S^{(i)}$ for each element of the structure using Eq. (18)
(11) Compute the internal force of each element $P^{(i)}$ using Eq. (19)
(12) Compute the vector of global internal nodal forces of each element $F^{(i)}$ using Eq. (20)
(13) Assemble the vector of global internal nodal forces of the entire structure.
(14) Perform optimization process and update the nodal displacement vector U
(15) Repeat step 7 to 15 until the convergence criterion is met
(16) Convergence criterion is not met at the buckling load. But the buckling load and its corresponding nodal displacements were already estimated using Eq. (22). After that, the upper and lower bounds of displacements are changed, and then $R^{(i+1)} = R^{(i)} + \lambda$.
(17) Repeat step 6 to 15 until the convergence criterion is met
(18) Dependent on the structure's inherent and its number of limit points, increasing and decreasing of the load may occur until the desired load or displacement is reached.

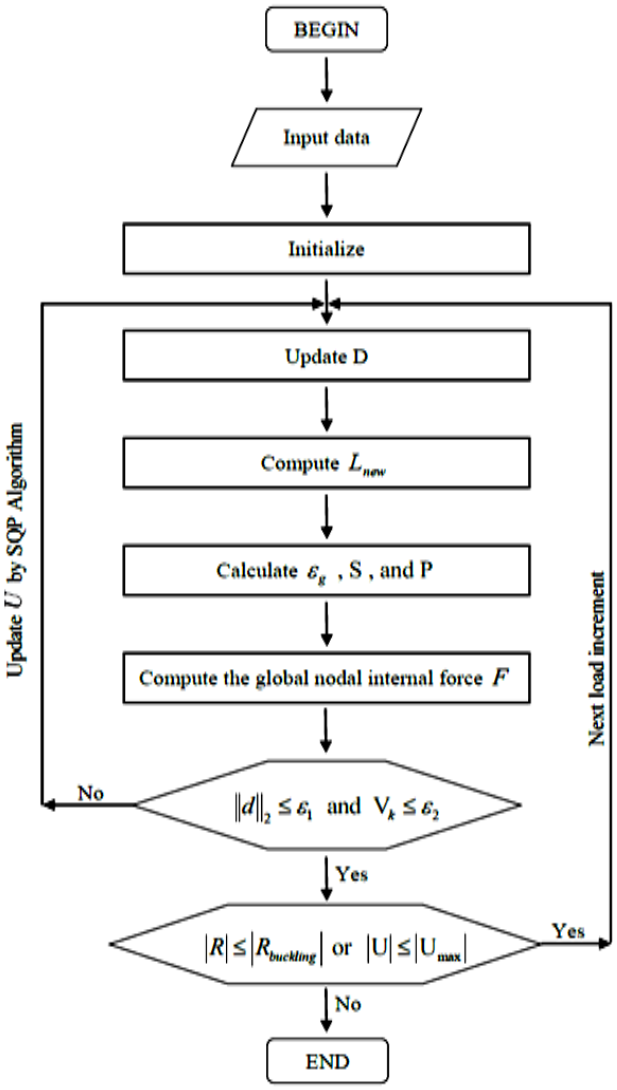

Fig. 2 Flowchart of the proposed algorithm

The whole analytical procedure is demonstrated as a flowchart in Fig. 2.

5. Numerical verifications

In this section, five plane truss structures are presented and studied to verify the efficiency and accuracy of the proposed approach. The results of these examples obtained by proposed method are compared to the outcomes of theoretical solution, modified arc-length method (Crisfield 1981 and Ramm 1981) using higher-order stiffness matrix, and other results reported in the literature. For all five truss structures, elastic geometrically nonlinear analysis is performed considering large deflections within the TL formulation framework. It should be stated that material nonlinearity, member and local buckling effects are not regarded in the examples.

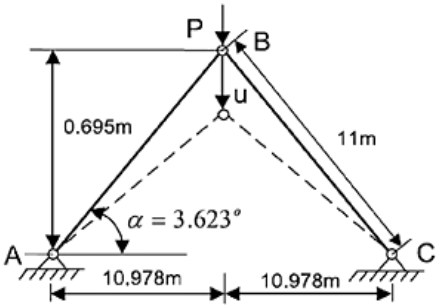

Fig. 3 Shallow truss (Torkamani and Shieh 2011)

Table 1 Geometric and mechanical characteristics of the shallow truss

Property	Value
Modulus of elasticity of each member	$E = 2.06\times10^7$ N/cm^2
Length of each member	$L = 11$ m $= 1100$ cm
Circular cross-section of each member	$A = 169$ cm^2
Rise angle	$\alpha = 3.623°$

Example 1: *shallow truss*

This structure is a two member truss that was previously investigated by Papadrakakis (1983) using dynamic relaxation method and also by Torkamani and Shieh (2011) using arc-length method. Fig. 3 shows the undeformed and deformed configuration of the truss with solid and dash lines, respectively.

The theoretical solution of this benchmark truss can be derived from Eq. (41)

$$P = \frac{2EA}{L}(h-u)\left[\left(1-\left(\frac{u}{L}\right)^2-\frac{2uh}{L^2}\right)^{-\frac{1}{2}}-1\right] \qquad (41)$$

Where, u is the vertical displacement of node B and h is the height of the truss before applying any load. The geometrical and mechanical properties of this example are presented in Table 1.

To follow the whole equilibrium path of the structure, two different cases are investigated. In Case 1, perfect model is regarded, but in Case 2, the cross-sectional area of the member BC is set to 10% smaller than the member AB to study the influence of geometrical imperfection. Fig. 4 depicts the vertical and horizontal load-displacement curve of node B.

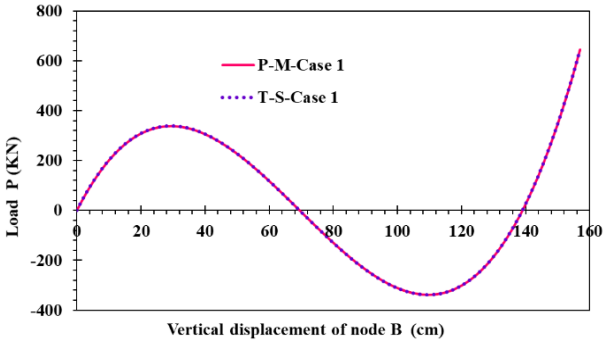

(a) Vertical displacement (Case 1)

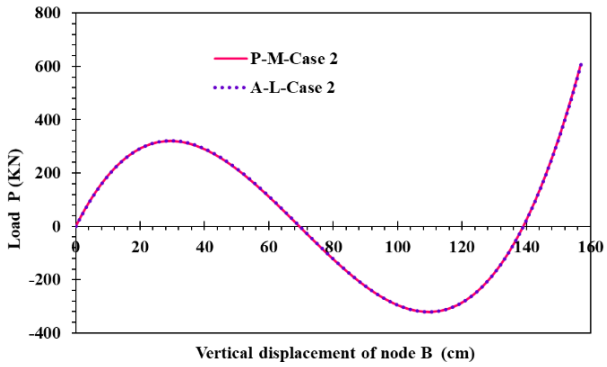

(b) Vertical displacement (Case 2)

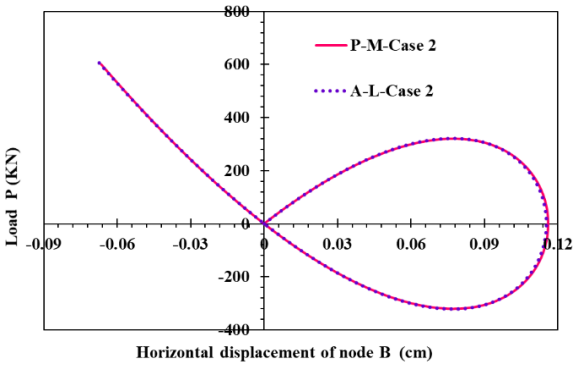

(c) Horizontal displacement (Case 2)

Fig. 4 Load-displacement curves of shallow truss

In Fig. 4(a), the results obtained by proposed method (P-M) are compared to those of theoretical solution (T-S)

Table 2 Analysis outcomes of the shallow truss

Case	Analysis type	First limit point		Second limit point	
		Limit load (KN)	u_B (cm)	Limit load (KN)	u_B (cm)
Case 1	T-S	338.79	29.39	-338.79	109.6
	P-M	338.5	29.37	-338.5	109.6
	Difference (%)	0.09	0.07	0.09	0
Case 2	P-M	321	29.3	-321	109.64
	A-L	321.3	28.67	-321.2	110.5
	Difference (%)	0.09	2	0.06	0.78

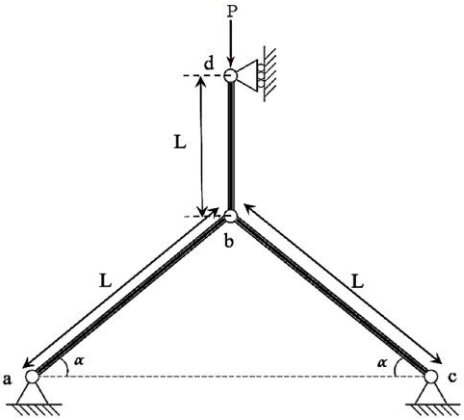

Fig. 5 Three member truss

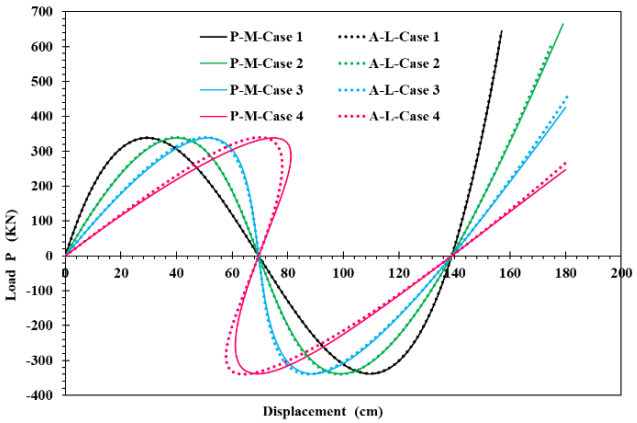

Fig. 6 Load-displacement curves of three member truss

derived by Eq. (41) for Case 1. In Figs. 4(b), (c), the results acquired by proposed method (P-M) are compared with modified arc-length method (A-L). The limit points obtained by proposed method, theoretical solution, and modified arc-length method are presented in Table 2.

It can be seen that the results acquired by proposed method have very good agreement with those generated by theoretical solution, and modified arc-length method. A typical snap-through and snap-back phenomena are exhibited in this example.

Example 2: *Three member truss*

In this example, a slightly more complex plane truss configuration is regarded. Another truss member is placed vertically on the top of the mentioned shallow truss. Fig. 5 shows the undeformed configuration of the truss. Both hinge points *b* and *d* are constrained to eliminate any horizontal displacement and thus they are only able to move vertically.

In fact, this problem has two degrees of freedom, and they are chosen to be the vertical displacements of nodes *b* and *d*. The influence of changing cross-sectional area of the member *bd* is studied in four cases to investigate the snap-through and snap-back phenomena. The geometrical and mechanical properties of the truss members are presented in Tables 3 for 4 different cases.

Fig. 6 shows the vertical load-displacement curve of node *d*.

The results obtained by proposed method (P-M) and modified arc-length (A-L) method are compared in this figure. The limit points generated by proposed method and modified arc-length method are presented in Table 4.

It can be seen that the results acquired by proposed method have good agreement with those obtained by modified arc-length method. For all cases, the limit loads derived by proposed method and modified arc-length method are 338.5 KN and 339.3 KN, respectively. The difference of limit loads generated by mentioned methods is 0.24%. A typical snap-through and snap-back phenomena are exhibited in this example.

Example 3: *Four member truss*

In this example, a variation of shallow truss is considered. Two truss members are attached horizontally on the top of the mentioned shallow truss. Fig. 7 shows the undeformed configuration of the four member plane truss.

Table 3 Properties of the three member truss

Case	Circular cross-section of member *bd* (A_{bd} (cm^2))	Circular cross-section of members *ab* and *bc* A_{ab} = A_{bc} (cm^2)	Modulus of elasticity E (N/cm^2)	L (cm)	α
Case 1	0	169	2.06×10^7	1100	3.623°
Case 2	1.69				
Case 3	0.845				
Case 4	0.4225				

Table 4 Properties of the three member truss

	Analysis type	First limit point				Second limit point			
		Case 1	Case 2	Case 3	Case 4	Case 1	Case 2	Case 3	Case 4
V_d (cm)	P-M	29.37	40.2	51.43	74.9	109.6	99	88	68.9
	A-L	29.4	39.92	50.2	70.4	109.37	98.6	87.8	64.5
	Difference (%)	0.1	0.7	2.4	6	0.2	0.4	0.23	6.4

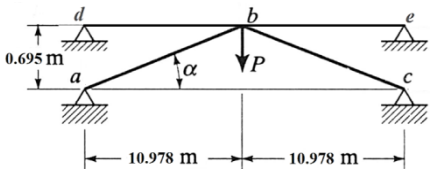

Fig. 7 Four member truss

The only degree of freedom is the vertical displacement of node *b*.

The influence of adding new members to the previous one is investigated in 6 cases. The geometrical and mechanical properties of the truss members are given in Table 5 for all 6 cases.

Fig. 6 shows the vertical load-displacement curve of node *b*.

The results acquired by proposed method (P-M) and modified arc-length (A-L) method are depicted in this figure for all 6 cases. The limit points derived by two mentioned methods are presented in Table 6.

It can be seen that the results acquired by proposed method agree well with those obtained by modified arc-length method. A typical snap-through phenomenon is exhibited in cases 1-4. It is noticeable that the more cross-sectional area is allocated to the members *db* and *be*, the more smooth load-displacement curve is achieved.

Example 4: *The reticulated* (*Thompson*) *strut*

The reticulated strut were analyzed for the first time by Thompson and Hunt (1973) and after that, by Kondoh and Atluri (1985) and Torkamani and Shieh (2011) to investigate different aspects of nonlinear analysis of the mentioned structure. The configuration of this structure is shown in

Table 6 Analysis outcomes of four member truss

C*	A-T*	First limit point		Second limit point	
		P (KN)	v_b (cm)	*P* (KN)	v_b (cm)
C-1*	P-M	338.5	29.4	-338.5	109.6
	A-L	339.3	29.85	-339.3	109.37
	D* (%)	0.24	1.5	0.24	0.2
C-2*	P-M	343.2	30	-155.1	100.9
	A-L	343.4	29.82	-158.3	99.4
	D* (%)	0.06	0.6	2	1.5
C-3*	P-M	351.52	31.1	99.2	85.1
	A-L	351.57	29.74	97.47	84.46
	D* (%)	0.01	4.3	1.7	0.75
C-4*	P-M	365.44	34.13	286.8	69.11
	A-L	366.58	35.24	286.24	68.66
	D* (%)	0.31	3.1	0.2	0.65
C-5*	P-M	-	-	-	-
	A-L	-	-	-	-
	D* (%)	-	-	-	-
C-6*	P-M	-	-	-	-
	A-L	-	-	-	-
	D* (%)	-	-	-	-

*C: Case 1; A-T: Analysis type; C-1: Case 1; C-2: Case 2; C-3: Case 3; C-4: Case 4; C-5: Case 5; C-6: Case 6; D: Difference

Table 5 Properties of the four member truss

Case	Circular cross-section of member *bd* and *be* (A_{bd} and A_{be} (cm^2))	Circular cross-section of members *ab* and *bc* A_{ab} = A_{bc} (cm^2)	Modulus of elasticity *E* (N/cm^2)	α
Case 1	0	169	2.06×10^7	3.623°
Case 2	10			
Case 3	30			
Case 4	55			
Case 5	90			
Case 6	140			

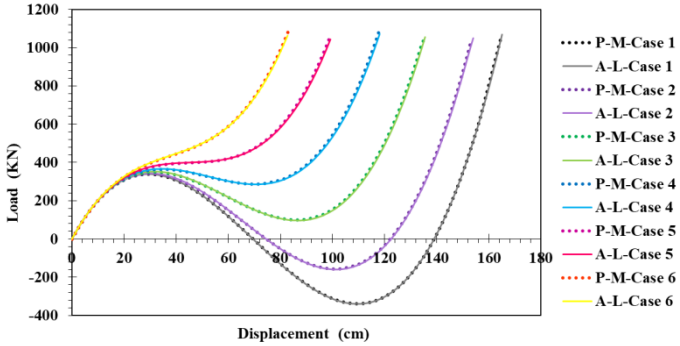

Fig. 8 Load-displacement curves of four member truss

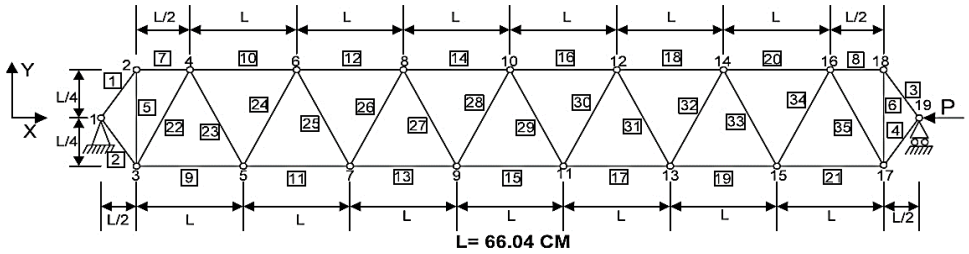

Fig. 9 The Thompson strut (Torkamani and Shieh (2011)

Fig. 9.

This structure consists of 35 members. The geometrical and mechanical properties of the truss members are given in Table 7.

This strut is subjected to a compressive load P at node 19. The load-displacement curve for the vertical displacement of node 10 is depicted in Fig. 10.

The buckling loads and the corresponding nodal displacements acquired by Kondoh and Atluri (1985), Torkamani and Shieh (2011), and proposed method (P-M) are presented in Table 8.

Table 7 Geometric and mechanical characteristics of the Thompson strut

Property	Value
Modulus of elasticity of each member	$E = 68.964\times10^5$ N/cm^2
Circular cross-section of member 1-21	$A = 54.84$ cm^2
Circular cross-section of member 22-35	$A = 51.61$ cm^2

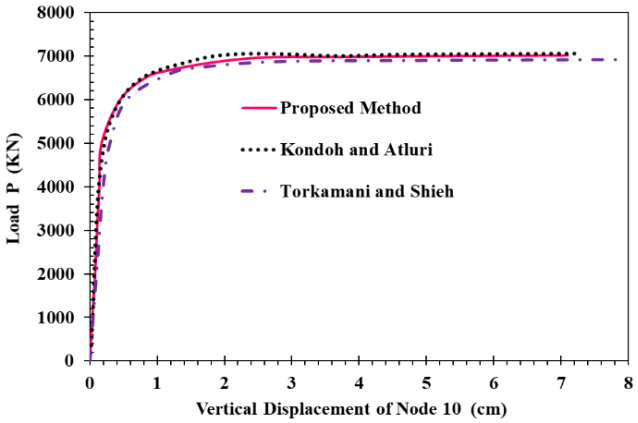

Fig. 10 Load-displacement curve for Thompson's strut

Table 8 Analysis outcomes of the Thompson strut

Solution method	Limit point	
	Limit load (KN)	Limit displacement (cm)
P-M	7014	7
Kondoh and Atluri (1985)	7063	7.22
Difference (%)	0.69	3
P-M	7014	7
Torkamani and Shieh (2011)	6916	8
Difference (%)	1.4	12.5

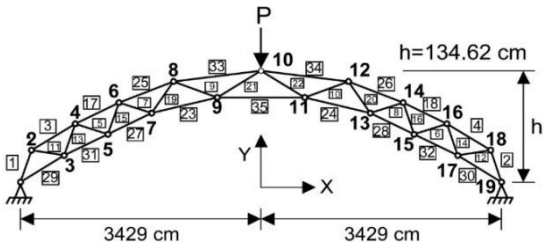

Fig. 11 The arch-truss structure (Torkamani and Shieh 2011)

Table 9 Nodal coordinates of the arch-truss structure (Kondoh and Atluri 1985)

Nodal number	X Coordinate (cm)	Y Coordinate (cm)
19,1	±3429	0
18,2	±3048	50.65
17,3	±2667	3475
16,4	±2286	83.82
15,5	±1905	65.3
14,6	±1524	110.85
13,7	±1143	87.99
12,8	±762	128.5
11,9	±381	100.65
10	0	134.6

Table 10 Cross-sectional areas of members of the arch-truss structure (Kondoh and Atluri 1985)

Member's number	Cross-section area (cm^2)
1-10,35	51.61
11,12	64.52
13-16	83.87
17,18	96.77
19-22	103.23
23,24	161.29
25,26	193.55
27,28	258.06
29-32	290.32
33,34	309.68

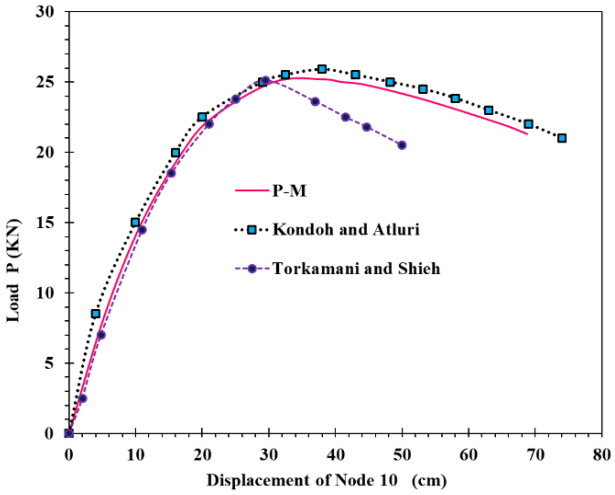

Fig. 12 Load-displacement curve of arch-truss structure for node (10) in vertical direction

Table 11 Analysis outcomes of the arch-truss structure

Solution method	Limit point	
	Limit load (KN)	Limit displacement (cm)
P-M	25.2	38
Kondoh and Atluri (1985)	25.89	38.1
Difference (%)	2.6	0.3
P-M	25.2	38
Torkamani and Shieh (2011)	25.11	29.5
Difference (%)	0.4	22.3

The generated results show good agreement for both limit load and its corresponding limit displacement.

Example 5: The Arch truss structure

The undeformed configuration of a 35-member plane arch-shape truss is shown in Fig. 11.

A vertical concentrated load P is applied at the node 10 of this truss. This structure was analyzed for the first time by Rosen and Schmit (1979), after that, Kondoh and Atluri (1985), and Torkamani and Shieh (2011) studied different aspects of the nonlinear analysis of the mentioned truss structure. In this problem, all of the members have a circular cross section and an identical modulus of elasticity of $E = 68.964\times10^5$ N/cm^2. The nodal coordinates of the structure and the cross-sectional areas for all of the members are presented in Tables 9 and 10, respectively.

Fig. 12 depicts the load-displacement curve of node 10 in the vertical direction corresponding to the applied load P.

The limit loads and the corresponding limit displacements generated by proposed method, Kondoh and Atluri (1985), and Torkamani and Shieh (2011) are presented in Table 11.

It can be seen that the outcomes of the proposed method are close to those of Kondoh and Atluri (1985) that used effective way of forming the tangent stiffness matrix of the truss and modified arch-length method, but the solution of the Torkamani and Shieh (2011) that used higher-order stiffness matrix and arch length method has become entirely divergent after the limit point.

6. Conclusions

In this research, a novel dual approach was developed to perform the geometrically nonlinear analysis of plane truss structures. For this purpose, an objective function was formed based on the classical stress-strain formulations, considering the entire higher-order terms. The proposed optimization problem was solved by SQP algorithm within the displacement-type constraints. The nonlinear equilibrium path of the plane truss structures was fully followed using the proposed method. It was shown that directly estimation of the critical loads and their corresponding limit points is possible by this method, and it is also applicable for problems having multiple limit points and exhibiting snap-through and snap-back phenomena. In addition, the present algorithm does not calculate any approximated stiffness matrix to form the main objective function, therefore, the errors caused by linearization of the equilibrium equation, and neglecting some of the nonlinear incremental strain components and higher-order terms will be eliminated from the obtained solution. Validity, efficiency and robustness of the suggested method was proved by means of the five numerical examples. It was confirmed that the present method can precisely predict the elastic pre- and post-buckling behavior of the plane truss structures.

References

Alnaas, W.F. and Jefferson, A.D. (2016), "A smooth unloading–reloading approach for the nonlinear finite element analysis of quasi-brittle materials", *Eng. Fract. Mech.*, **152**, 105-125.

Arora, J.S. (2012), *Introduction to Optimum Design*, (Third Edition), Academic Press, Boston, MA, USA.

Baguet, S. and Cochelin, B. (2003), "On the behaviour of the ANM continuation in the presence of bifurcations", *Commun. Numer. Methods Eng.*, **19**(6), 459-471.

Bathe, K.-J. (2006), *Finite Element Procedures*, Klaus-Jurgen Bathe.

Bathe, K.-J. and Dvorkin, E.N. (1983), "On the automatic solution of nonlinear finite element equations", *Comput. Struct.*, **17**(5), 871-879.

Belegundu, A.D. and Arora, J.S. (1984a), "A Computational Study of Transformation Methods for Optimal Design", *AIAA J.*, **22**(4), 535-542.

Belegundu, A.D. and Arora, J.S. (1984b), "A recursive quadratic programming method with active set strategy for optimal design", *Int. J. Numer. Methods Eng.*, **20**(5), 803-816.

Bellini, P. and Chulya, A. (1987), "An improved automatic incremental algorithm for the efficient solution of nonlinear finite element equations", *Comput. Struct.*, **26**(1), 99-110.

Bhatti, M.A. (2006), *Advanced Topics in Finite Element Analysis of Structures: With Mathematica and MATLAB Computations*, John Wiley & Sons, Inc.

Chen, W.-F. and Lui, E.M. (1991), *Stability Design of Steel Frames*, CRC press.

Crisfield, M.A. (1981), "A fast incremental/iterative solution procedure that handles "snap-through"", *Comput. Struct.*, **13**(1),

55-62.
Crisfield, M. (1983), "An arc-length method including line searches and accelerations", *Int. J. Numer. Methods Eng.*, **19**(9), 1269-1289.
Crisfield, M.A. (1991), *Nonlinear Finite Element Analysis of Solids and Structures. Vol. 1*: *Essentials*, John Wiley & Sons.
Damil, N. and Potier-Ferry, M. (1990), "A new method to compute perturbed bifurcations: application to the buckling of imperfect elastic structures", *Int. J. Eng. Sci.*, **28**(9), 943-957.
Elhage-Hussein, A., Potier-Ferry, M. and Damil, N. (2000), "A numerical continuation method based on Padé approximants", *Int. J. Solids Struct.*, **37**(46), 6981-7001.
Felippa, C.A. (2001), "Nonlinear finite element methods", *Aerospace Engineering Sciences Department of the University of Colorado. Boulder*.
Forde, B.W. and Stiemer, S.F. (1987), "Improved arc length orthogonality methods for nonlinear finite element analysis", *Comput. Struct.*, **27**(5), 625-630.
Garcea, G., Madeo, A., Zagari, G. and Casciaro, R. (2009), "Asymptotic post-buckling FEM analysis using corotational formulation", *Int. J. Solids Struct.*, **46**(2), 377-397.
Geers, M.-a. (1999), "Enhanced solution control for physically and geometrically non-linear problems. Part I—the subplane control approach", *Int. J. Numer. Methods Eng.*, **46**(2), 177-204.
Hamdaoui, A., Braikat, B. and Damil, N. (2016), "Solving elastoplasticity problems by the Asymptotic Numerical Method: Influence of the parameterizations", *Finite Elem. Anal. Des.*, **115**, 33-42.
Hellweg, H.-B. and Crisfield, M. (1998), "A new arc-length method for handling sharp snap-backs", *Comput. Struct.*, **66**(5), 704-709.
Izadpanah, M. and Habibi, A. (2015), "Evaluating the spread plasticity model of IDARC for inelastic analysis of reinforced concrete frames", *Struct. Eng. Mech., Int. J.*, **56**(2), 169-188.
Jiang, G., Li, F. and Li, X. (2016), "Nonlinear vibration analysis of composite laminated trapezoidal plates", *Steel Compos. Struct., Int. J.*, **21**(2), 395-409.
Kondoh, K. and Atluri, S. (1985), "Influence of local buckling on global instability: Simplified, large deformation, post-buckling analyses of plane trusses", *Comput. Struct.*, **21**(4), 613-627.
Liang, K., Ruess, M. and Abdalla, M. (2014), "The Koiter–Newton approach using von Kármán kinematics for buckling analyses of imperfection sensitive structures", *Comput. Methods Appl. Mech. Eng.*, **279**, 440-468.
Liang, K., Ruess, M. and Abdalla, M. (2016), "Co-rotational finite element formulation used in the Koiter–Newton method for nonlinear buckling analyses", *Finite Elem. Anal. Des.*, **116**, 38-54.
Mahdavi, S.H., Razak, H.A., Shojaee, S. and Mahdavi, M.S. (2015), "A comparative study on application of Chebyshev and spline methods for geometrically non-linear analysis of truss structures", *Int. J. Mech. Sci.*, **101**, 241-251.
Mansouri, I. and Saffari, H. (2012), "An efficient nonlinear analysis of 2D frames using a Newton-like technique", *Arch. Civil Mech. Eng.*, **12**(4), 485-492.
Papadrakakis, M. (1983), "Inelastic post-buckling analysis of trusses", *J. Struct. Eng.*, **109**(9), 2129-2147.
Pastor, M.M., Bonada, J., Roure, F. and Casafont, M. (2013), "Residual stresses and initial imperfections in non-linear analysis", *Eng. Struct.*, **46**, 493-507.
Planinc, I. and Saje, M. (1999), "A quadratically convergent algorithm for the computation of stability points: The application of the determinant of the tangent stiffness matrix", *Comput. Methods Appli. Mech. Eng.*, **169**(1), 89-105.
Powell, M.J. (1978), "A fast algorithm for nonlinearly constrained optimization calculations", In: *Numerical Analysis*, Springer, pp. 144-157.
Ramm, E. (1981), "Strategies for tracing the nonlinear response near limit points", In: *Nonlinear Finite Element Analysis in Structural Mechanics*, Springer, pp. 63-89.
Rao, S.S. (2009), *Engineering Optimization*: *Theory and Practice*, John Wiley & Sons.
Rezaiee-Pajand, M. and Naserian, R. (2017), "Nonlinear frame analysis by minimization technique", *Iran Univ. Sci. Technol.*, **7**(2), 291-318.
Rezaiee-Pajand, M., Salehi-Ahmadabad, M. and Ghalishooyan, M. (2014), "Structural geometrical nonlinear analysis by displacement increment", *Asian J. Civil Eng.* (*BHRC*), **15**(5), 633-653.
Riks, E. (1972), "The application of Newton's method to the problem of elastic stability", *J. Appl. Mech.*, **39**(4), 1060-1065.
Riks, E. (1979), "An incremental approach to the solution of snapping and buckling problems", *Int. J. Solids Struct.*, **15**(7), 529-551.
Rosen, A. and Schmit, L.A. (1979), "Design-oriented analysis of imperfect truss structures—part I—accurate analysis", *Int. J. Numer. Methods Eng.*, **14**(9), 1309-1321.
Saada, A.S. (2013), *Elasticity*: *Theory and Applications*, Elsevier.
Saffari, H. and Mansouri, I. (2011), "Non-linear analysis of structures using two-point method", *Int. J. Non-Linear Mech.*, **46**(6), 834-840.
Saffari, H., Mansouri, I., Bagheripour, M.H. and Dehghani, H. (2012), "Elasto–plastic analysis of steel plane frames using Homotopy Perturbation Method", *J. Constr. Steel Res.*, **70**, 350-357.
Schweizerhof, K. and Wriggers, P. (1986), "Consistent linearization for path following methods in nonlinear FE analysis", *Comput. Methods Appl. Mech. Eng.*, **59**(3), 261-279.
Thai, H.-T. and Kim, S.-E. (2009), "Large deflection inelastic analysis of space trusses using generalized displacement control method", *J. Constr. Steel Res.*, **65**(10-11), 1987-1994.
Thompson, J.M.T. and Hunt, G.W. (1973), *A General Theory of Elastic Stability*, John Wiley & Sons.
Torkamani, M.A. and Shieh, J.-H. (2011), "Higher-order stiffness matrices in nonlinear finite element analysis of plane truss structures", *Eng. Struct.*, **33**(12), 3516-3526.
Torkamani, M.A. and Sonmez, M. (2008), "Solution techniques for nonlinear equilibrium equations", *Proceedings of 18th Analysis and Computation Specialty Conference* (*ASCE*), Vancouver, BC, Canada, April.
Wan, C.-Y. and Zha, X.-X. (2016), "Nonlinear analysis and design of concrete-filled dual steel tubular columns under axial loading", *Steel Compos. Struct., Int. J.*, **20**(3), 571-597.
Wempner, G.A. (1971), "Discrete approximations related to nonlinear theories of solids", *Int. J. Solids Struct.*, **7**(11), 1581-1599.
Yang, Y.-B. and Kuo, S.-R. (1994), "Theory and analysis of nonlinear framed structures."

CC